Hybrid imaging using linear retroreflectors

Lorne Whitehead, Alexandra Kushnir, and Peter Kan

It has been observed that retroreflective materials can be used in combination with beam splitters to produce real images. This is practical on a large size scale but has a maximum optical efficiency of 25%. Conversely, curved reflectors efficiently produce real images, but their cost increases very rapidly with size. We introduce a new imaging method, which combines the advantages of both systems, through the use of a linear retroreflective film. This material is retroreflective in one plane and conventionally reflective in the perpendicular plane. The net result is an efficient real image system that can have unlimited extent in one transverse direction, and which can be inexpensively manufactured on a large scale. © 2006 Optical Society of America

OCIS codes: 260.0260, 260.6970.

1. Introduction

A conventional retroreflector directs incident light back in the direction from which it came, an effect that is very useful for making objects highly conspicuous in the beam of automobile headlights. Retroreflectors are now ubiquitous, found in products ranging from highway signs to running shoes. Typically, they use spherical lenses or corner reflectors to achieve the retroreflective effect.

Although very well known in this conspicuity application, retroreflectors also have a less well-known attribute—they can be used to form real 3D images without the use of conventional lenses or mirrors.[1,2] This is achieved in the arrangement shown in Fig. 1, in which a beam splitter is used in combination with a retroreflective sheet.

Although this arrangement has the disadvantage of low optical efficiency (less than 25%), it has some very interesting advantages. In principle, the image is clear and undistorted, three dimensional, and in focus everywhere. Moreover, the image can be large relative to the optical path length. These features are very difficult to achieve with conventional lenses and mirrors, and so one might expect this imaging method to have numerous applications. However, little practical use has been made of this effect, probably mainly because of the low efficiency. This paper introduces a new imaging system, which captures many of the advantages of retroreflective images, while achieving very high efficiency.

2. Imaging With Linear Retroreflectors

Linear retroreflectors would appear to offer some opportunity for creating images. Such a material is commercially available in the form of a prismatic polycarbonate sheet,[3] as shown in Fig. 2, in which the reflection mechanism is total internal reflection. (This material is normally used to make prism light guides.[4])

As shown in Fig. 3, most of the light incident on the smooth side of this film reflects in a direction lying in the plane containing the prisms' longitudinal direction and the incident ray, with the angle between the ray and the prisms' longitudinal direction preserved. In other words, the material behaves as a mirror with regard to motion in the prism longitudinal direction, and as a retroreflector for motion perpendicular to the prism longitudinal direction.

Figure 4 shows the linear focusing effect of a small portion of flat retroreflector sheet.[5] (For clarity only the reflective back of the prismatic structure is shown in Fig. 4, and the prism size is exaggerated.) As shown, the retro imaging effect causes the diverging rays from a source to converge along a line focus that is parallel to the direction of the retroreflector prisms, and passing through the source. This focusing effect is not perfect, just as with conventional retroreflective images, because of the finite size of the retroreflective prisms, angular imperfections, and diffraction, but these effects are not too serious with available materials.

The authors are with the Department of Physics and Astronomy, University of British Columbia, 6224 Agricultural Road, Vancouver, British Columbia, V6T 1Z1, Canada. L. Whitehead's e-mail address is lorne.whitehead@ubc.ca.

Received 4 January 2006; revised 9 April 2006; accepted 14 April 2006; posted 17 April 2006 (Doc. ID 66847).

0003-6935/06/276998-07$15.00/0

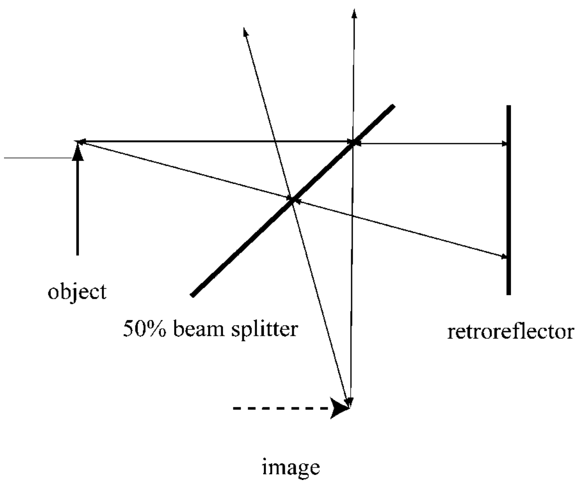

Fig. 1. Method of producting real images with a retroreflective sheet.

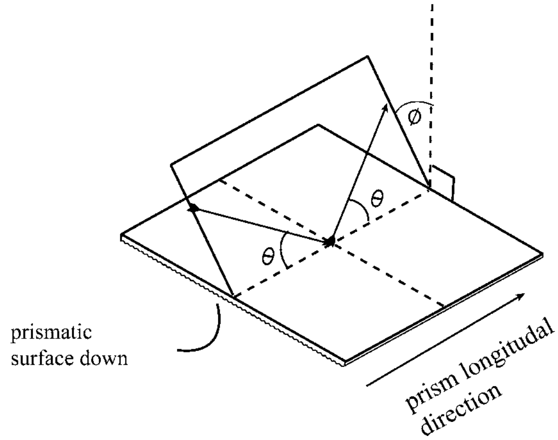

Fig. 3. Reflection direction from a linear retroreflector.

Figure 5 shows the linear focusing effect of a small portion of cylindrically curved conventional mirror material. As shown, the surface curvature causes the diverging rays from a source to converge along a line focus that is parallel to the axis of the cylinder. In this arrangement, the dimensions are related by the relation

$$\frac{1}{s_o} + \frac{1}{s_i} = \frac{2}{r\cos(\phi)}. \qquad (1)$$

As the arrangement in Fig. 4 produces a horizontal line focus, and that of Fig. 5 produces a vertical line focus, it is interesting to consider whether a combination of the two could produce a point focus. The available retroreflective sheet is easily deformed into a smooth curve, so this combination is readily achieved, as shown in Fig. 6.

In order for the two line focuses to coincide, it is apparent from Fig. 4 that s_o must equal s_i, and thus from Eq. (1) we can deduce that this hybrid focusing effect works provided that

$$s_o = s_i = r\cos(\phi). \qquad (2)$$

It is interesting to note that Eq. (2) describes a cylindrical surface whose cross section corresponds to the well-known Rowland circle associated with a mirror having a circular cross section.[6] This system is efficient, and the object and the image can extend unlimitedly in a direction perpendicular to the optical axis. We believe this to be the first optical system with this combination of characteristics. However, there are three disadvantages with this system. First, imaging is possible only for object points lying on a surface; namely those on the cylinder mentioned above. Second, the effective optical axis is not, in general, perpendicular to this image surface. Third, there is an aberration associated with the curved retroreflector, which becomes unacceptable as the physical extent of the retroreflector becomes significant relative to s_o.

As shown in an exaggerated manner in Fig. 7, rays that strike the nearest portion of the retroreflector reach their retroreflective focus too soon, and similarly, those striking the most distant portion focus too late. This aberration severely limits the acceptable size of the reflector in some imaging applications.

3. Applications

It is interesting, however, that this limitation does not preclude the creation of good real image displays based on this concept, as shown in the photograph in Fig. 8. In this particular setup, the image was simply photographed using a 35 mm camera, with no need for any kind of imaging screen. The image is located at a well-defined 3D position, and is sharp even

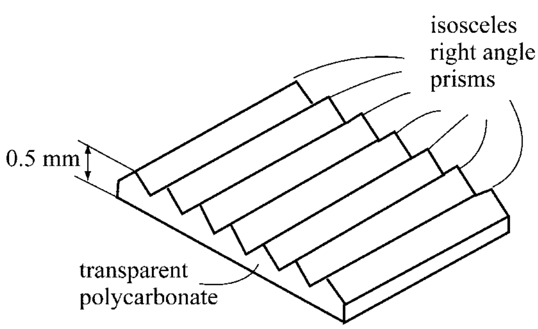

Fig. 2. Commercially available linear retroreflector.

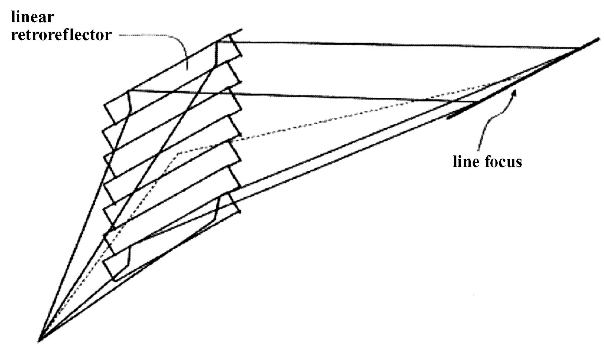

Fig. 4. Linear focusing effect of a flat linear retroreflector.

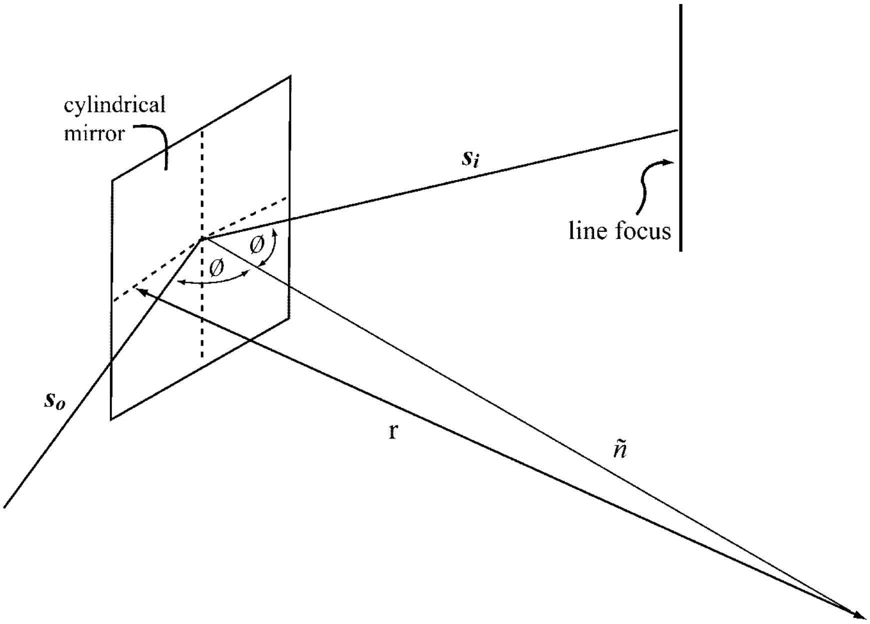

Fig. 5. Linear focusing effect of a cylindrically curved mirror.

though a large curved retroreflector is used. The reason that the aberration of Fig. 7 does not cause a problem in Fig. 8 is that only a small portion of the retroreflector is involved in imaging any given portion of the object. Actually, the aberration does alter the relationship of the object and image surfaces, but this is easily corrected by slight adjustment of the location of the object. In the photograph, at any given point in the object, only a small region of the retroreflector is responsible for reflecting those rays that eventually reach the eye. The arrangement of the components photographed in Fig. 8 is shown in Fig. 9. Although the simple hybrid system of Fig. 9 has imaging capabilities, it is interesting to consider whether it might be possible to overcome the retroreflective imaging aberration described above, and to image a volumetric region of object points, as required for true 3D imaging.

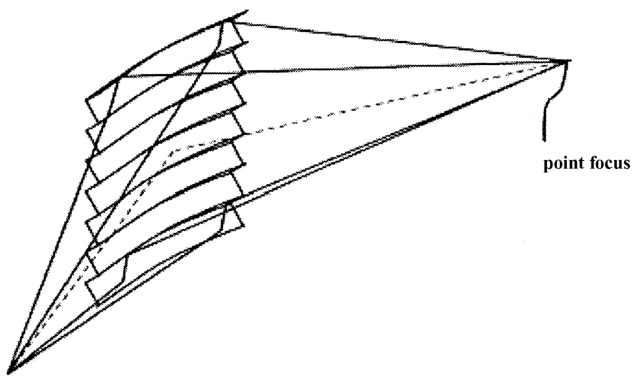

Fig. 6. Point focus achieved with cylindrically curved linear retroreflective film.

At this point it is helpful to recall the well-known optical characteristics of a pair of identical confocal converging lenses, as shown in Fig. 10. In this arrangement, an object is at the external focus of the first lens, and is imaged with negative one magnification at the external focus of the second lens. This

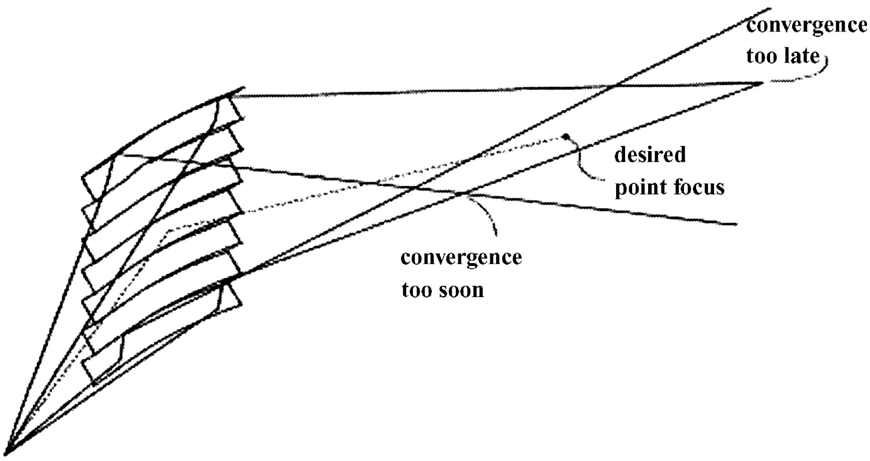

Fig. 7. Significant aberration associated with curved retroreflection.

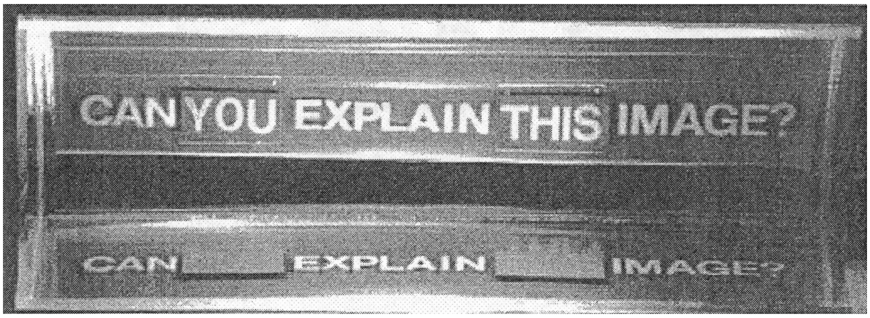

Fig. 8. Photo of simple demonstration of a hybrid real image. In the top sentence, the words "you" and "this" are real objects, and the words "can," "explain," and "image" are real images of the corresponding objects below.

occurs because the first lens collimates the light from an object point in a direction determined by the location in the object plane, and the second lens focuses the collimated light to a point in the image plane determined by the direction of the collimated light. Such a system reproduces not only the spatial intensity distribution of the object plane, but also the angular distribution of that light as well, which means that a 3-space of object points is reproduced without distortion in the image space.[7] This effect has been referred to as a "telewindow,"[8] as it effectively reproduces a visual field at a displaced location.

Figure 11 depicts an analogous structure based on off-axis retroreflectors. As shown, the distance from the object to the mirror is the effective focal length at angle ϕ, which is $(r/2)\cos\phi$, about $0.35r$ in the case where ϕ is 45°. The reflected light is collimated in the plane of Fig. 11. (Of course, this is perfectly true only if the mirror is a parabola with focus at the object point. We will ignore the cylindrical aberration, as it is a small correction relative to the main retroreflective aberration we are trying to correct.) In the out-of-plane direction, the light passes through a retroreflective line focus between the two mirrors, and then expands out again. Because of the retroreflective aberration effect, this line focus is steeply inclined, as shown in Fig. 11. The purpose of this arrangement is to use a second retroreflective focusing step to allow reconvergence to a point. By symmetry, it can be shown that the light diverging from this retroreflective line focus is ideally directed so that it will reconverge at a point focus after reflecting off the second retroreflector. The result is that the light focuses, in this approximation, to a good point focus at the effective focal point of the second retroreflector.

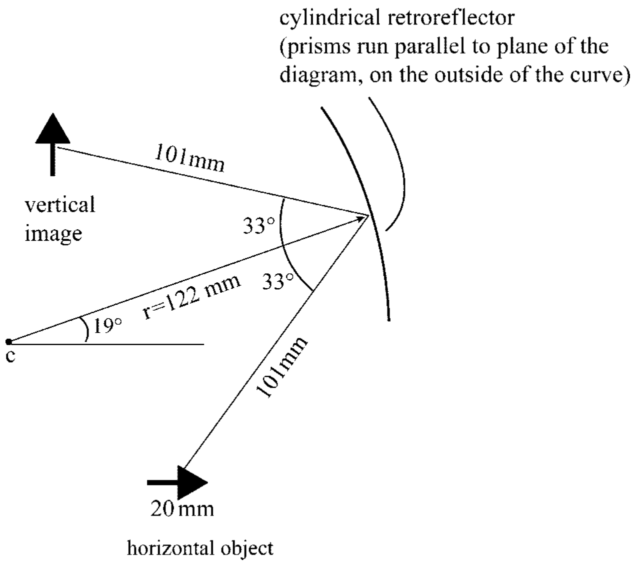

Fig. 9. Cross section of scene photographed in Fig. 8.

4. Experimental Setup

To quantitatively evaluate the quality of the optical image, an experiment based on the arrangement in Fig. 11(b) was performed. For the purposes of this demonstration, the reflectors were shaped as segments of a parabola having a focal length of 48.5 mm. To ensure the correct focusing behavior, the center point of the two reflectors (which were identical in shape) was selected as the point on the parabolic curve that is located a distance of $2f$ from the focal point (F) such that an angle of $\phi = 45°$ is formed between the parabola and a line perpendicular to the axis running through the parabola's vertex. Figure 12 shows the reflector portion, highlighted in bold, relative to the larger parabola.

The bases for holding the reflectors were machined from a thick sheet of acrylic, to a finished size of approximately 100 mm $\times$ 100 mm. They were lined with a flexible layer of linear retroreflector, with the linear prisms oriented perpendicular to the z axis and with the size and shape as shown in Fig. 13. For measurement purposes, the object was a 0.40 mm aperture, illuminated with a high brightness fiber optic illuminator having an approximately Lambertian output. The resulting image was projected onto a 60 μm thick plastic diffuser screen. To quantify the quality of the image, images were taken using several different exposure values with a digital camera. The resulting images were combined into a single high dynamic range image using customized software[9]

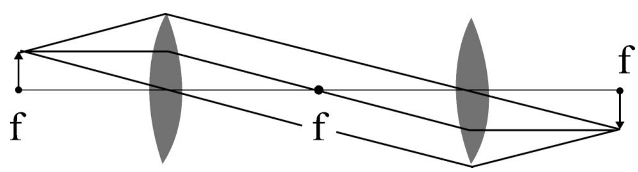

Fig. 10. Imaging with confocal lenses.

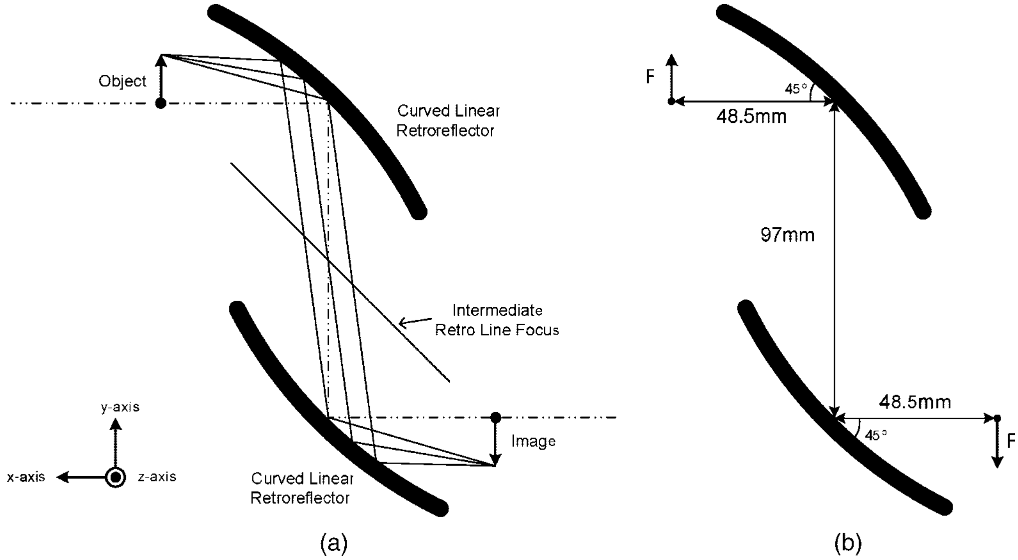

Fig. 11. Improved imaging with two cylindrical retroreflectors: (a) retroreflectors collimate light; (b) schematic of the proportions of the hybrid imaging system.

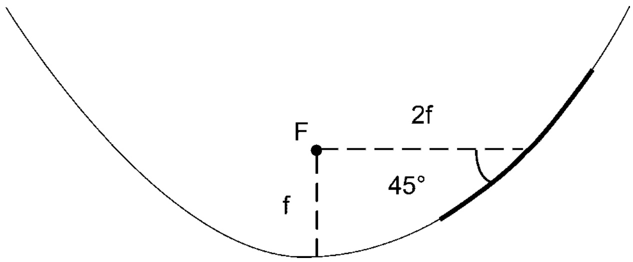

Fig. 12. Retroreflector as part of a parabola (retroreflector is bold).

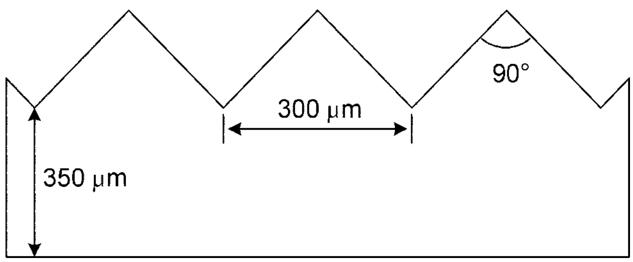

Fig. 13. Dimensions of a linear retroreflector.

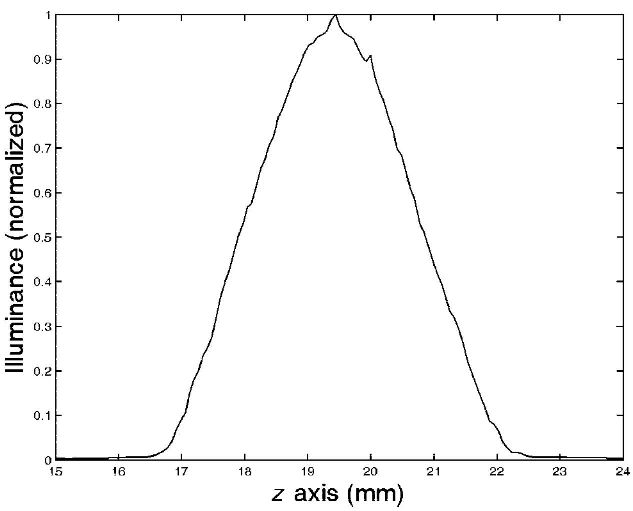

Fig. 14. Image plot using the hybrid system.

and converted into calibrated luminance data files. The quality of the image was found to be remarkably good, when compared to the object. Figure 14 shows the plot of the image.

The FWHM is 3 mm, which, while larger than that of the object, is small enough to yield meaningful images on a large size scale. This is comparable to the estimated blur size, Δx, resulting purely from diffraction and the lateral displacement within the prisms, which is given roughly by

$$\Delta x = 2\left(\frac{2\lambda\bar{L}}{w} + 2w\right), \tag{3}$$

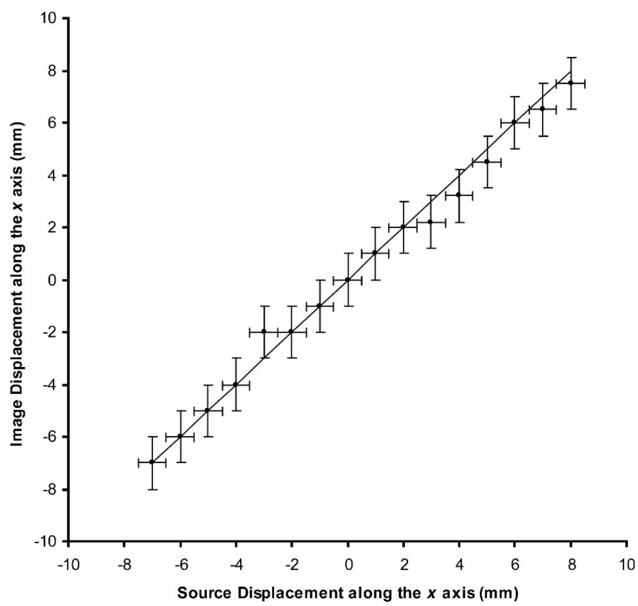

Fig. 15. x axis displacement of image as the source is moved along the x axis.

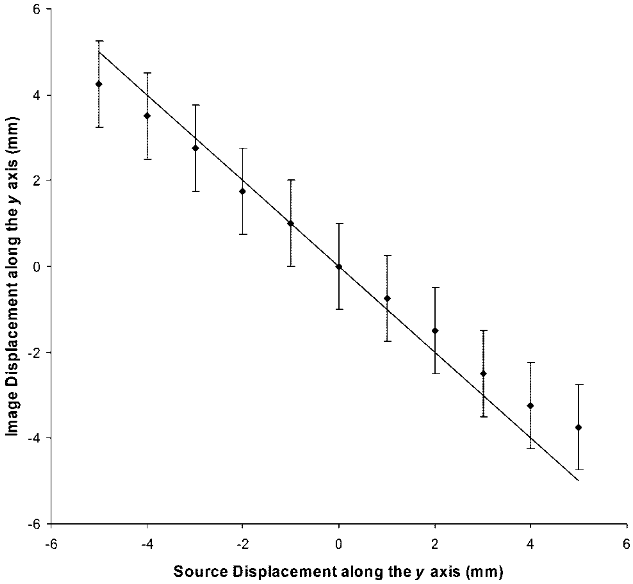

Fig. 16. y axis displacement of image as the source is moved along the y axis.

where $\bar{L}$ is the mean distance from the prism to the image (48.5 mm), w is the prism width (0.3 mm), and λ is the wavelength of the light (550 nm), yielding an approximate predicted value of 1.5 mm.

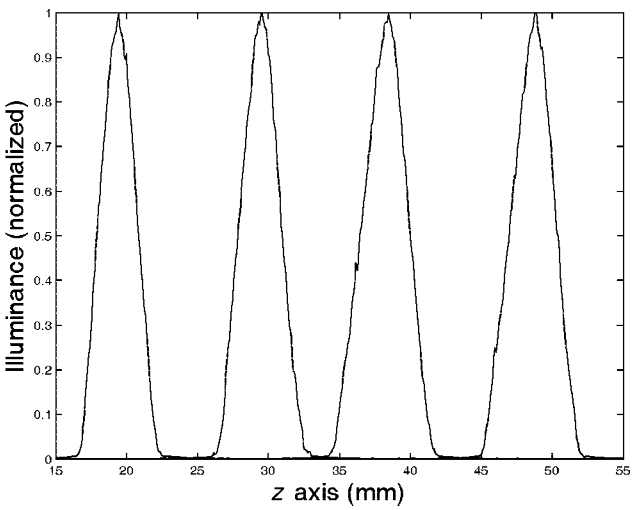

Fig. 17. Movement of the image along the z axis.

Using the arrangement shown in Fig. 11(b), three different tests were preformed. First, the object was moved incrementally along the x axis of the system and the position of the focused image was recorded, by moving the diffuse screen to the position of maximum image sharpness. This experiment determines the extent to which the system exhibits unity magnification, since it is expected that when the object is moved, the image focus will move in the same direction and by the same magnitude.

Figure 15 shows the measured displacement of the focused image as a function of the object's position along the x axis, where the error bars were determined by the spread in a series of measurements at the same position. The line shown is the prediction based on the assumption of unity gain, which is completely consistent with the bulk of the actual data points. An acceptable image with only slight aberration was attained within a span of 45% of the focal length.

Similarly, the same procedure was followed for the y axis. In this case, it was not necessary to move the screen to the position of maximum sharpness, as this plane remained constant throughout the entire procedure. Figure 16 shows the displacement of the focused image as a function of the object's position along the y axis. In this case, the slope of the fit is -1, as would be expected in this geometry. An acceptable image with only slight aberration was attained within a span of 10% of the focal length.

Finally, we considered displacements of the object along the z axis. As expected, as the object was moved along the z axis, the image position experienced a comparable motion along the z axis. This behavior is demonstrated in Fig. 17, in which the object was sequentially moved by 10 mm increments in the z direction; as expected, the widths of the various peaks do not change, nor does their spacing. The unlimited extent of imaging in the z direction is a most satisfying feature of this system. Of course this system still contains numerous remaining aberrations, but for a reasonable image size these can be about the same size as the fundamental limitations of the retroreflector arising from finite prism size and diffraction. Overall, a reasonably convincing 3D image is possible. A further advantage is that this can be made inexpensively on a large size scale, as demonstrated by the three different views in Fig. 18, of an

Fig. 18. Three views of a full size 3D image of a person made by two off-axis confocal cylindrical linear retroreflectors.

image of a person produced by this method. The image itself was magnification 1, but of course the photograph in Fig. 18 is reduced for this paper.

5. Conclusion

It would appear that curved linear retroreflectors offer a new imaging system with interesting properties. In particular, it is encouraging that the object can be large relative to the optical path length, and optical efficiency is still very high. Further, it is very easy to fabricate the required structure by curving an available linear retroreflector, so low cost, large-scale applications are possible. However, several limitations should also be noted. The magnification must always be unity, and the object distance and image distance must be equal. Further, the image clarity is poorer than with real lenses, due to diffraction and errors in the retroreflector. Based on these observations, it is suggested that further study in this area is warranted.

The authors are very grateful to Ric Dreyer, 3M Company, for sharing his insights on the retroreflective imaging properties of linear retroreflectors. His enthusiasm for this concept is largely responsible for the work reported here. Similarly, Lee Palmer of Simon Fraser University is thanked for his interest in the pedagogical value of nontraditional imaging techniques, including retroreflective imaging. The authors also gratefully acknowledge the funding of this work by the 3M Company, and by the Natural Sciences and Engineering Research Council of Canada.

References

1. J. Walker, "The amateur scientist: wonders with the retroreflector, a mirror that removes distortion from a light beam," Sci. Am., **254,** 118–123 (1986).
2. S. F. Jacobs, "Experiments with retro-directive arrays," Opt. Eng. **21,** 281–283 (1982).
3. 3M Optical Lighting Film™ Product No. 2301, manufactured by 3M Company, St. Paul, Minn. 55144.
4. L. A. Whitehead, R. A. Nodwell, and F. L. Curzon, "New efficient light guide for interior illumination," Appl. Opt. **21,** 2755–2757 (1982).
5. Ric Dreyer, 3M Center, Building 235, St. Paul, Minnesota 55144 (personal communication, 1999).
6. M. Born and E. Wolf, *Principles of Optics,* 7th ed. (Cambridge U. Press, 2002), p. 459.
7. V. Mahajan, in *Optical Imaging and Aberration: Part I* (SPIE Optical Engineering Press, 1998), pp. 348–364.
8. M. A. Duguay, G. D. Aumiller, "Transmission of 3D images by means of lens guides," Appl. Opt. **18,** 2081–2084 (1979).
9. PHOTOSPHERE HIGH DYNAMIC RANGE IMAGE software, Anyhere Software, Albany, California 94706-2358.